Journal of Virology

Ultradeep Pyrosequencing Detects Complex Patterns of CD8$^+$ T-Lymphocyte Escape in Simian Immunodeficiency Virus-Infected Macaques

Benjamin N. Bimber, Benjamin J. Burwitz, Shelby O'Connor, Ann Detmer, Emma Gostick, Simon M. Lank, David A. Price, Austin Hughes and David O'Connor

J. Virol. **2009, 83(16):8247. DOI: 10.1128/JVI.00897-09. Published Ahead of Print 10 June 2009.**

JOURNAL OF VIROLOGY, Aug. 2009, p. 8247–8253 Vol. 83, No. 16
0022-538X/09/$08.00+0 doi:10.1128/JVI.00897-09

NOTES

Ultradeep Pyrosequencing Detects Complex Patterns of CD8$^+$ T-Lymphocyte Escape in Simian Immunodeficiency Virus-Infected Macaques$^{\nabla}$†

Benjamin N. Bimber,[1]‡ Benjamin J. Burwitz,[2]‡ Shelby O'Connor,[2]‡ Ann Detmer,[1] Emma Gostick,[3] Simon M. Lank,[1] David A. Price,[3] Austin Hughes,[4] and David O'Connor[1,2]*

Wisconsin National Primate Research Center, University of Wisconsin—Madison, Madison, Wisconsin 53706[1]; Department of Pathology and Laboratory Medicine, University of Wisconsin—Madison, Madison, Wisconsin 53706[2]; Department of Medical Biochemistry and Immunology, Cardiff University School of Medicine, Heath Park, Cardiff, United Kingdom[3]; and Department of Biological Sciences, University of South Carolina, Columbia, South Carolina 29208[4]

Received 5 May 2009/Accepted 1 June 2009

Human and simian immunodeficiency viruses (HIV/SIV) exhibit enormous sequence heterogeneity within each infected host. Here, we use ultradeep pyrosequencing to create a comprehensive picture of CD8$^+$ T-lymphocyte (CD8-TL) escape in SIV-infected macaques, revealing a previously undetected complex pattern of viral variants. This increased sensitivity enabled the detection of acute CD8-TL escape as early as 17 days postinfection, representing the earliest published example of CD8-TL escape in intrarectally infected macaques. These data demonstrate that pyrosequencing can be used to study the evolution of CD8-TL escape during immunodeficiency virus infection with an unprecedented degree of sensitivity.

Rapid sequence evolution is a hallmark of immunodeficiency virus infection and represents a major obstacle toward the development of a successful human immunodeficiency virus (HIV) vaccine (2, 3). Viral evolution has implications for HIV treatment and provides critical information about host immune responses. Although the viral population contains an enormous amount of sequence diversity, standard sequencing methods are limited to the detection of high-frequency variants. Techniques that permit characterization of rare variants, such as molecular cloning, single-genome amplification, or quantitative RT-PCR, are either labor intensive or restricted to the detection of a single variant, limiting their widespread use (9, 11, 12, 18). As a result, the functional consequences of low-frequency variants and subtle differences in the kinetics of viral evolution are not well understood.

CD8$^+$ T lymphocytes (CD8-TL) play a critical role in the suppression of immunodeficiency viruses and are a driving force in HIV/SIV (simian immunodeficiency virus) viral evolution (7, 8, 15, 20). Because the emergence of escape mutations within CD8-TL epitopes alters the recognition of infected cells, monitoring viral variation within epitopes has important implications (10, 16). Due to the sequencing limitations noted above, studies of CD8-TL escape are generally limited to the detection of high-frequency variants. As a result, CD8-TL escape is frequently viewed as a binary event: an epitope is either wild type or escaped.

In this study, we applied ultradeep pyrosequencing to evaluate acute CD8-TL escape in SIV-infected macaques. We validated this method by sequencing the Tat_{28-35}SL8 (SL8) epitope in eight Indian rhesus macaques, demonstrating the ability to detect amino acid variants with a frequency as low as 1%. We then examined $Nef_{103-111}$RM9 (RM9) viral escape in four Mauritian cynomolgus macaques (MCMs), demonstrating that viral escape within RM9 occurs as early as 17 days postinfection. Pyrosequencing detected a considerable heterogeneity in the diversity, frequency, and kinetics of viral variation between animals that was undetectable by conventional methods. This exceptional variability is present in the viral population until at least 20 weeks postinfection. These studies demonstrate that ultradeep pyrosequencing is a high-throughput method that can be used to sensitively detect and characterize CD8-TL escape variants in any given epitope.

Ultradeep pyrosequencing of Tat_{28-35}SL8 in SIV-infected Indian rhesus macaques. We initially applied pyrosequencing to study SIVmac239 escape in the well-characterized Mamu-A1*001-restricted epitope Tat_{28-35}SL8 (SL8) (note: following revisions in macaque major histocompatibility complex [MHC] nomenclature, the allele formerly published as *Mamu-A*01* will be referred to as *Mamu-A1*001* [19]). Viral RNA samples from four SIV-infected, *Mamu-A1*001*-positive and four SIV-infected, *Mamu-A1*001*-negative animals were isolated from plasma at weeks 1, 2, 3, 4, 8, and 20 postinfection. Three of the *Mamu-A1*001*-positive animals (rh2122, rh2126, and rh2127) were vaccinated with a DNA prime/recombinant modified vaccinia virus Ankara regimen prior to intrarectal SIVmac239

* Corresponding author. Mailing address: University of Wisconsin—Madison, 555 Science Drive, Madison, Wisconsin 53711. Phone: (608) 890-0845. Fax: (608) 265-8084. E-mail: doconnor@primate.wisc.edu.

† Supplemental material for this article may be found at http://jvi.asm.org/.

‡ These authors contributed equally to the manuscript.

$^{\nabla}$ Published ahead of print on 10 June 2009.

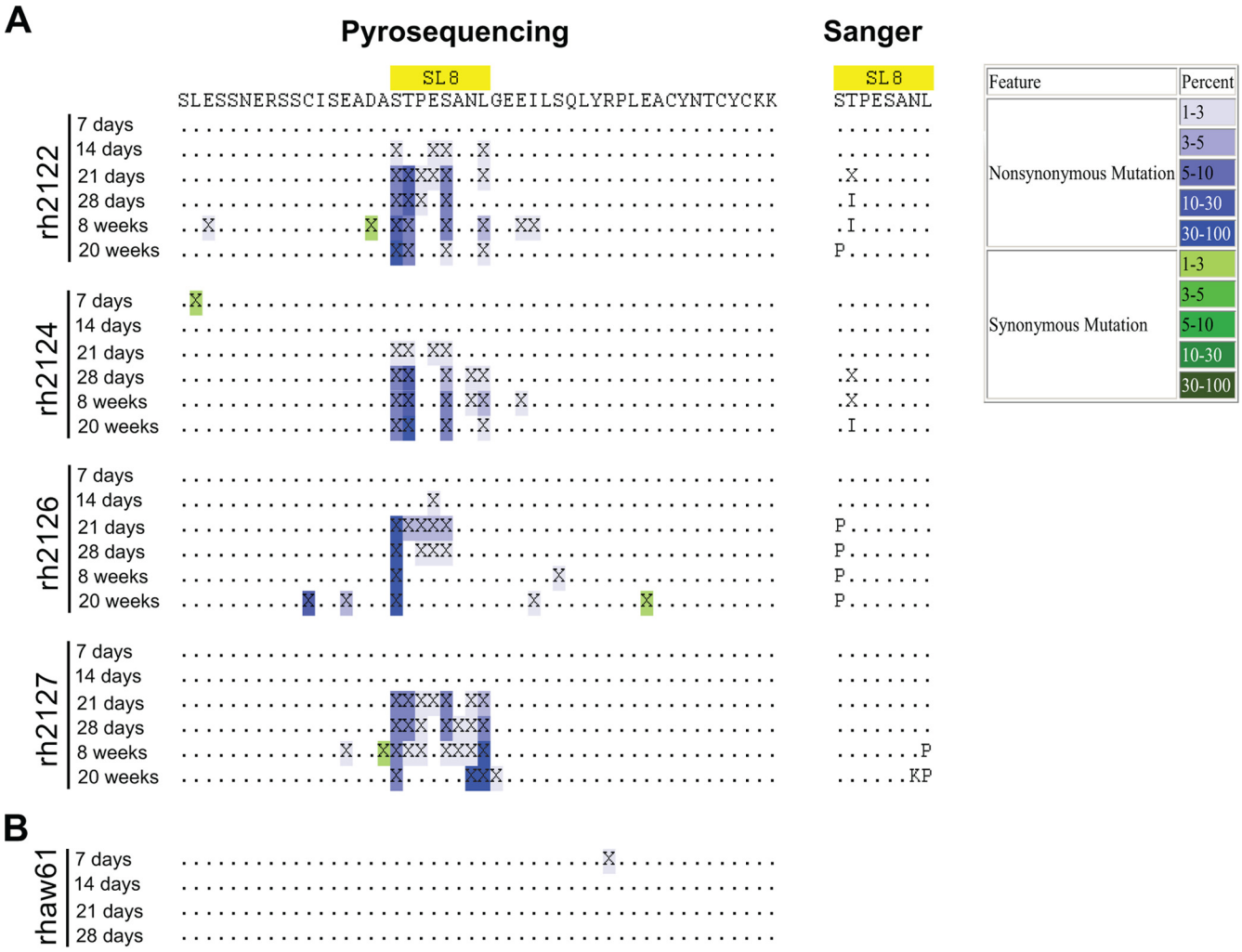

C

Sequence	Animal (21 days post infection)			
STPESANL	rh2122	rh2124	rh2126	rh2127
....	23.6	79.8	6.9	26.6
P.......	14.3	3.1	58.9	19.2
.I......	31.5	5.2	0.9	17.9
....L...	17.5	2.1	5.2	13.8
..S.....	0.2	0.6	5.8	2.0
F.......	0.2	0.7	3.5	1.8
.A......	1.2	0.7	3.1	0.5
.N......	0.2	--	4.0	0.1
...K....	0.2	0.7	3.0	1.1
...G....	1.2	1.3	2.0	--
..L.....	2.0	0.2	0.6	2.5
.......R	1.2	0.3	0.5	2.9
.......P	0.9	0.8	0.3	2.8
Other	5.8	4.6	5.5	8.7
Sanger Seq.	.X......	....	P.......	....

D

Sequence	Animal (20 weeks post infection)			
STPESANL	rh2122	rh2124	rh2126	rh2127
P.......	80.7	17.5	96.5	5.5
......KP	--	--	--	71.5
.I......	10.6	56.4	--	--
....	6.6	8.4	1.0	7.1
....L...	0.9	9.6	--	--
P.....KP	--	--	--	4.7
.......T	--	--	--	4.2
P......P	--	--	--	3.9
.N......	--	3.0	--	--
.......P	0.9	--	--	1.2
.......R	--	1.0	--	0.4
.I..L...	--	1.3	--	--
Other	0.4	2.8	2.5	1.4
Sanger Seq.	P.......	.I......	P.......	......KP

FIG. 1. Sequencing of Tat_{28-35}SL8 in rhesus macaques. The Tat_{28-35}SL8 regions from four *Mamu-A1*001*-positive rhesus macaques were sequenced using both pyrosequencing and conventional Sanger sequencing. (A) Consensus sequence from each sample with any change indicated as X. The pyrosequencing consensus (left) contains any mutation present in 1% or more of the total reads. Nonsynonymous and synonymous mutations are colored according to prevalence, indicated by the color key in the upper right. The consensus sequence obtained from conventional Sanger sequencing is displayed on the right. (B) Pyrosequencing consensus sequence from a *Mamu-A1*001*-negative animal, showing all mutations present at greater than 1%. (C) Percentage of each variant observed by pyrosequencing at day 21 within Tat_{28-35}SL8. Only variants present at 1% or greater in at least one animal are shown. All other variants are expressed as "Other." Dashes indicate that a variant was not present in that sample. (D) Similar to panel C, showing variants at week 20.

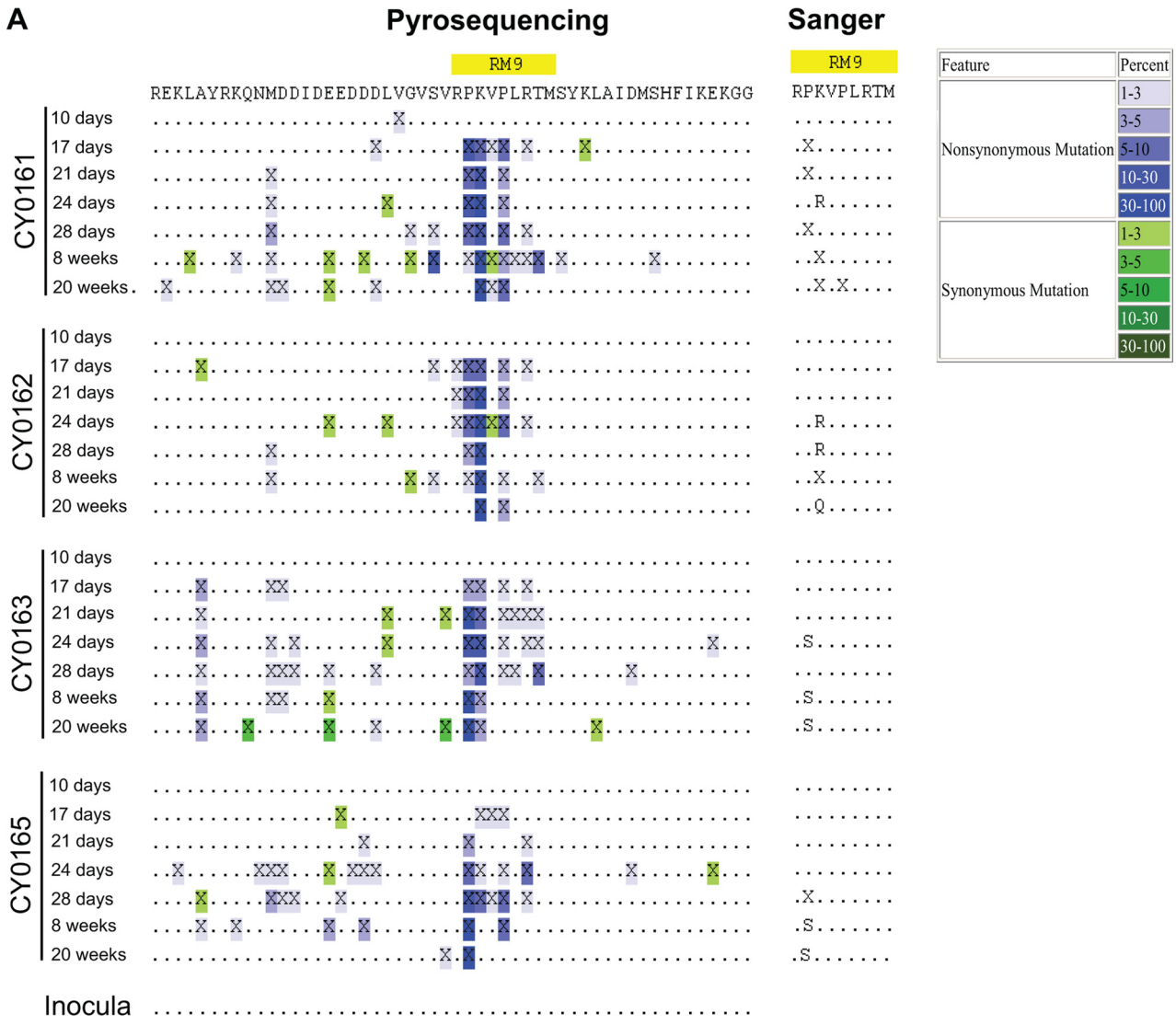

B

Sequence	Animal (17 days post infection)			
RPKVPLRTM	CY0161	CY0162	CY0163	CY0165
....	20.6	15.4	10	87.4
.S.......	24.3	8.4	50.3	6.7
..R......	31.8	46.2	22.1	0.6
....S....	4.8	2	2	0.7
....L....	1.9	3.3	0.5	---
..Q......	1.5	2.1	0.9	---
.T.......	1.8	2.7	0.8	---
......K..	0.2	0.3	0.8	2
..N......	0.6	1.3	0.2	---
K........	0.4	2.1	0.4	0.3
..T......	0.5	1.6	---	---
..K......	0.1	---	0.1	---
.......P.	---	---	1.8	---
.....Q...	0.2	0.7	1	---
Other	11.4	13.9	9.1	2.3
Sanger Sequence	..R......	..R......	.S.......	....

C

Sequence	Animal (20 weeks post infection)			
RPKVPLRTM	CY0161	CY0162	CY0163	CY0165
....	4.4	12.2	2.4	0.04
.S.......	---	---	84.9	94.3
..R......	0.4	---	---	---
....S....	14.7	9.3	---	---
..Q......	61.9	78.1	5.6	---
....A....	6.9	---	---	---
..NS.....	1.7	---	---	---
Other	10.1	0.4	7.1	5.7
Sanger Sequence	..X.X....	..Q......	.S.......	.S.......

FIG. 2. Sequencing of $Nef_{103-111}$RM9 in MCMs. The $Nef_{103-111}$RM9 regions from four *Mafa-A1*063*-positive MCMs were sequenced using both pyrosequencing and conventional Sanger sequencing. A SIVmac239 inoculum was also sequenced by pyrosequencing. (A) Consensus sequence from each sample with any change indicated as X. The pyrosequencing consensus (left) contains any mutation present in 1% or more of total sequence reads. An average of 1,008 reads was obtained for each sample, with greater than 350 reads obtained from all samples except for cy0161 at day 17 (203 reads) and cy0162 at week 20 (237 reads). Nonsynonymous and synonymous mutations are colored according to prevalence, indicated by the color key in the upper right. The consensus sequence obtained from conventional Sanger sequencing is displayed on the right. (B) Percentage of each variant observed by pyrosequencing at day 17 within $Nef_{103-111}$RM9. Only variants present at 1% or greater in at least one animal are shown. All other variants are expressed as "Other." Dashes indicate that a variant was not present in that sample. (C) Similar to panel B, showing variants at week 20.

infection (21). The generation and pyrosequencing of RT-PCR amplicons is described in detail in the methods section of the supplemental material. Previous studies using pyrosequencing to study HIV drug resistance have demonstrated that approximately 400 reads are needed to detect nucleotide variants at a frequency of greater than 1% in nonhomopolymeric regions (22). We obtained an average of 1,707 reads per sample, with a minimum of 455. Therefore, we are likely able to detect most of the major amino acid variants in each sample.

Figure 1A contains the consensus sequence of each sample, showing positions with mutations present in greater than 1% of the viral population. The pattern of mutation is more comprehensive than that obtained by conventional Sanger sequencing of bulk PCR products (Fig. 1A). While it is not currently known at what threshold a low-frequency mutation should be considered biologically relevant, it is worth noting that of the amino acid mutations not detected by conventional Sanger sequencing, 22 were present in 10% or more of the population. We observed variation within SL8 in all *Mamu-A1*001*-positive animals by day 21, with low-frequency variants appearing at day 14 in two of four animals. The kinetics of escape are consistent with previously published findings using Sanger sequencing of bulk PCR products or individual viral clones (1, 13, 16). To ensure the accuracy of this technique, we included multiple controls. As might be expected, we did not observe any mutations at week 1, except for a single low-frequency synonymous mutation in rh2124. Further, there was a significant decrease in the frequency of mutations observed in the region flanking the SL8 epitope compared with the number of mutations within the epitope (see Table S2 in the supplemental material). As a control, we sequenced the same region from the SIVmac239 inoculum and from four SIV-infected *Mamu-A1*001*-negative rhesus macaques (Fig. 1B and Fig. S1 in the supplemental material). Neither the inoculum nor the *Mamu-A1*001*-negative macaques had detectable mutations in the SL8 epitope. Together, these data strongly suggest that the variation we observed is a direct consequence of CD8-TL pressure and that pyrosequencing can accurately detect mutations present with a frequency as low as 1%.

Unlike conventional sequencing of bulk PCR products, pyrosequencing provides clonal sequences, enabling the characterization of individual variants (Fig. 1C and D; also see Tables S3 to S6 in the supplemental material). A total of 13 distinct sequence variants were observed in SL8 at day 21 (Fig. 1C). Interestingly, there was considerable heterogeneity in both the diversity and frequency of variants among the *Mamu-A1*001*-positive animals, continuing to at least 20 weeks postinfection (Fig. 1D). Thus, we demonstrate that even though a mutation may appear fixed by Sanger sequencing, extensive variability can remain within the viral population. These differences in the timing, pattern, and frequency of viral variants may influence disease outcome, yet they are rarely studied because existing methods for examining this variation are extremely labor intensive.

Ultradeep pyrosequencing of $Nef_{103\text{-}111}$RM9 in SIV-infected MCMs. We next used pyrosequencing to examine viral escape in a group of four MCMs. Unlike the rhesus macaques in the previous section, all MCMs were unvaccinated and infected intrarectally with 50,000 50% tissue culture infectious doses of SIVmac239. Using methods similar to our SL8 analysis, we prepared and sequenced RT-PCR amplicons spanning the *Mafa-A1*063*-restricted epitope $Nef_{103\text{-}111}$RM9 (RM9) (4) (see Table S1 in the supplemental material). Following revised nomenclature, the allele formerly published as *Mafa-A*25* will be referred to as *Mafa-A1*063*.

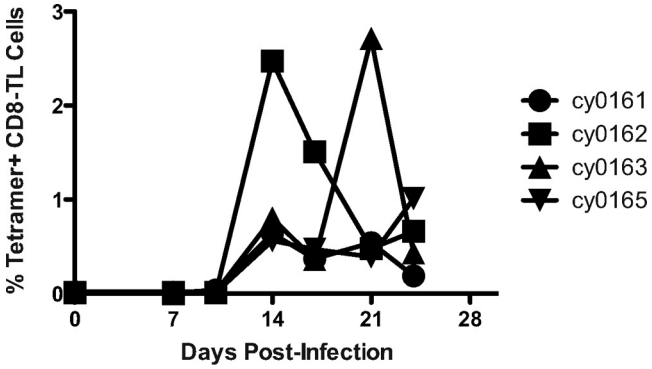

FIG. 3. Data represent the percentage of tetramer-positive cells within the $CD3^+$ $CD8^+$ cell gate. The limit of detection was 0.02% as determined by day 0 postinfection tetramer staining.

As with SL8, we found considerable heterogeneity in patterns of viral variation within the RM9 epitope (Fig. 2A; also see Tables S7 to S11 in the supplemental material). Remarkably, we detected amino acid variation within RM9 by 17 days postinfection in all four MCMs. The majority of these sequence variants represent less than 20% of the viral population (Fig. 2B) (17). More than 50% of the sequences obtained from CY0162 at 17 days postinfection contained one or more variant amino acids within this epitope (Fig. 2C). These data imply that CD8-TL selection occurs as early as 17 days postinfection. While CD8-TL escape mutations have been detected in SL8 between 13 and 20 days after intravenous SIV infection (13), the appearance of viral variants earlier than 3 weeks after intrarectal SIV infection in unvaccinated animals has not yet been reported. Unlike the case with Tat SL8, there was a considerable number of low-frequency mutations in the region flanking RM9. Because SIVmac239 was isolated following passage through rhesus macaques, we cannot rule out the hypothesis that these mutations represent species-specific viral adaptations. All four MCMs expressed *Mafa-A1*063*, so we also cannot rule out the possibility that this adaptation is MHC specific. However, it is worth noting that unlike RM9, Tat SL8 is located within the overlapping reading frames of Tat and Vpr. Therefore, one might hypothesize that mutations within SL8 are more likely to result in loss of fitness, decreasing the plasticity of this region (6).

Tetramer analysis of $Nef_{103\text{-}111}$RM9-specific CD8-TL. We measured the frequency of peripheral RM9-specific CD8-TL to confirm that the expansion of this population was associated with the appearance of viral variants. Frozen peripheral blood mononuclear cell samples from each animal were simultaneously thawed and stained with the MHC

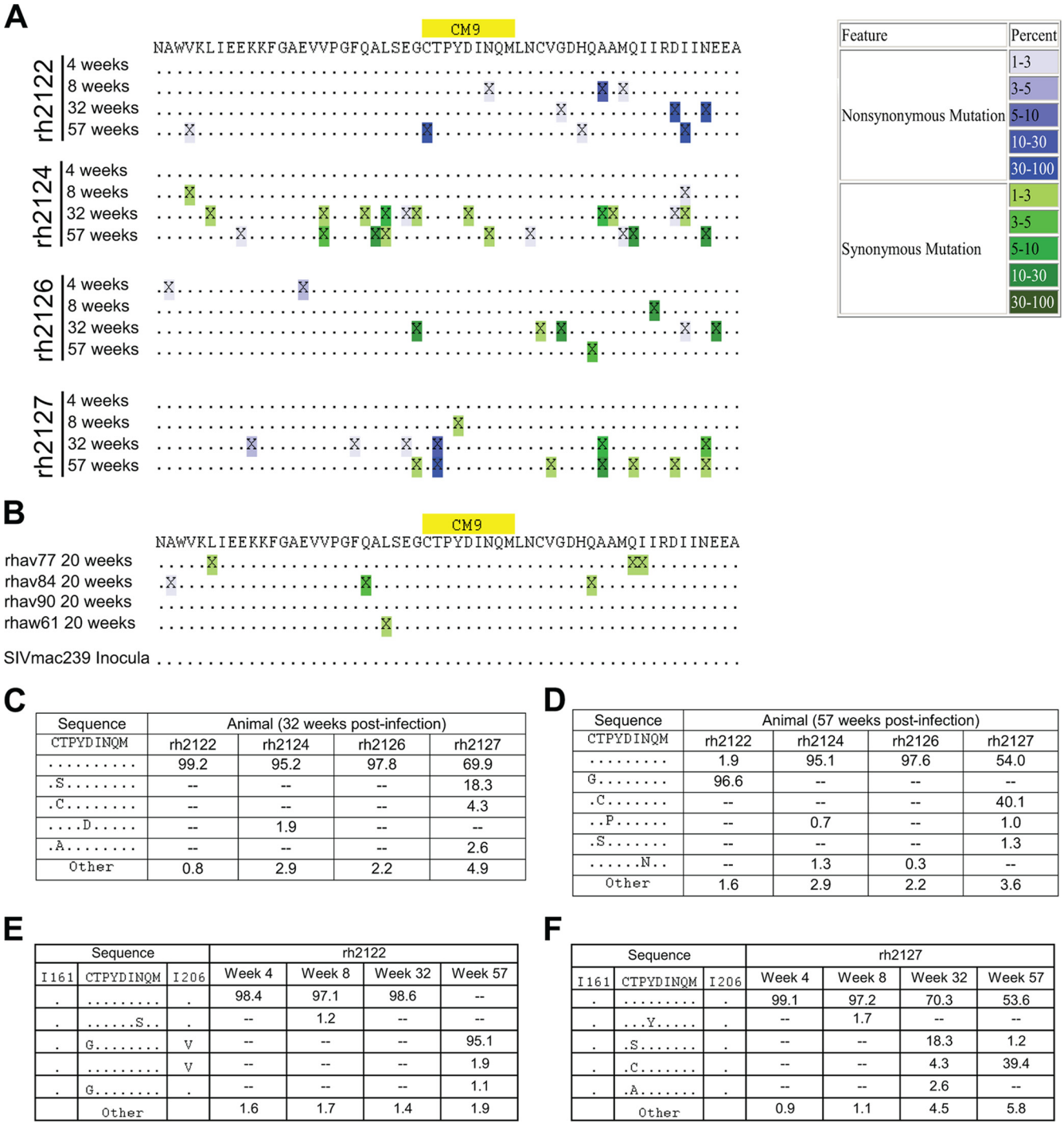

C

Sequence	Animal (32 weeks post-infection)			
CTPYDINQM	rh2122	rh2124	rh2126	rh2127
....	99.2	95.2	97.8	69.9
.S.....	--	--	--	18.3
.C.....	--	--	--	4.3
....D....	--	1.9	--	--
.A.....	--	--	--	2.6
Other	0.8	2.9	2.2	4.9

D

Sequence	Animal (57 weeks post-infection)			
CTPYDINQM	rh2122	rh2124	rh2126	rh2127
....	1.9	95.1	97.6	54.0
G.....	96.6	--	--	--
.C.....	--	--	--	40.1
..P.....	--	0.7	--	1.0
.S.....	--	--	--	1.3
.....N..	--	1.3	0.3	--
Other	1.6	2.9	2.2	3.6

E

Sequence			rh2122			
I161	CTPYDINQM	I206	Week 4	Week 8	Week 32	Week 57
.	....	.	98.4	97.1	98.6	--
.	.....S..	.	--	1.2	--	--
.	G.....	V	--	--	--	95.1
.	....	V	--	--	--	1.9
.	G.....	.	--	--	--	1.1
	Other		1.6	1.7	1.4	1.9

F

Sequence			rh2127			
I161	CTPYDINQM	I206	Week 4	Week 8	Week 32	Week 57
.	....	.	99.1	97.2	70.3	53.6
.	...Y.....	.	--	1.7	--	--
.	.S.....	.	--	--	18.3	1.2
.	.C.....	.	--	--	4.3	39.4
.	.A.....	.	--	--	2.6	--
	Other		0.9	1.1	4.5	5.8

FIG. 4. Sequencing of $Gag_{181-189}$CM9 in Indian rhesus macaques. The $Gag_{181-189}$CM9 region from four *Mamu-A1*001*-positive Indian rhesus macaques was sequenced by pyrosequencing. (A) Consensus sequence from each sample with any change indicated as X. The pyrosequencing consensus (left) contains any mutation present in 1% or more of total reads. Nonsynonymous and synonymous mutations are colored according to prevalence, indicated by the color key in the upper right. (B) Pyrosequencing consensus sequence from four *Mamu-A1*001*-negative animals and a SIVmac239 inoculum, showing all mutations present at greater than 1%. (C) Percentage of each variant observed by pyrosequencing at week 32 within $Gag_{181-189}$CM9. Only variants present at 1% or greater in at least one animal are shown. All other variants are expressed as "Other." Dashes indicate that a variant was not present in that sample. (D) Similar to panel C, showing variants at week 57. (E) Table showing the linkage between $Gag_{181-189}$CM9 variants and known compensatory mutations at amino acid positions 161 and 206 for animal rh2122. (F) Similar to panel E, showing data for rh2127.

class I tetramer Mafa-A1*063 Nef RM9-APC, CD8-PerCP, and CD3-FITC. In all four MCMs, we identified tetramer-positive CD8-TL in the periphery beginning at 14 days postinfection (Fig. 3), comparable to the kinetics of an SL8 CD8-TL response (1, 14). These data strongly support our pyrosequencing results and suggest that selective pressure exerted by SIVmac239-specific CD8-TL leads to variation within RM9.

Ultradeep pyrosequencing of $Gag_{181-189}$CM9 in SIV-infected Indian rhesus macaques. Next we examined viral escape within $Gag_{181-189}$CM9 (CM9), a well-characterized Mamu-A1*001-restricted epitope that generally does not escape until chronic infection (5). By week 57, we only observed CM9 escape in rh2122 and rh2127 (Fig. 4A). Examination of variant frequency revealed CM9 mutation by week 32 in rh2127; however, the wild-type sequence remained dominant through week 57 (Fig. 4C and D). In contrast, no CM9 mutation was observed in rh2122 until after week 32; however, a variant containing C181G comprised 96.6% of the population by week 57 (Fig. 4C and D).

Several compensatory mutations have been associated with CM9 escape, including I161V and I206V (5, 23). Variants with I161V were not observed in any animal (data not shown). In rh2122, 95.1% of variants with C181G also contained I206V (Fig. 4E). In contrast, I206V is never observed in rh2127, an animal in which escape variants never comprise more than 50% of the population; however, we cannot rule out the existence of additional compensatory mutations outside this amplicon (Fig. 4F). For additional sequence data from weeks 4 and 8, see Tables S12 and S13 in the supplemental material.

Application of ultradeep pyrosequencing to the entire SIV genome. With the success of sequencing individual amplicons, we tested whether this method could be applied to the entire viral genome. We designed 32 overlapping amplicons of approximately 400 bp each, spanning SIVmac239 from nucleotides 1077 to 10267 (see Table S14 in the supplemental material). We then performed RT-PCR on RNA isolated from a SIVmac239 stock. These overlapping reads were assembled to produce an average of 562-fold coverage at each nucleotide position, although coverage was variable across the genome (see Fig. S2A in the supplemental material). Within the coding regions, we detected only nine point mutations present in 1% or greater of the viral population, with no mutation present at greater than 1.6% (see Fig. S2B in the supplemental material). These results demonstrate that ultradeep pyrosequencing of amplicons can be applied to sequencing the entire SIV genome and represent the most rigorous characterization of the homogeneity of a SIVmac239 stock.

The data presented here demonstrate exceptional complexity within SIV epitopes recognized by CD8-TL using ultradeep pyrosequencing. The ability to readily identify and quantify viral variants should permit unprecedented assessment of variant ontogeny, allowing a more nuanced view of the selection, reversion, and potential fitness of variants that arise during HIV/SIV infection.

This work was supported by R21 AI068488-02 and R01 AI077376 by the NIH. Support to A.H. was provided by grant number GM43940 by the NIH. D.A.P. is a Medical Research Council (MRC) UK Senior Clinical Fellow. This publication was made possible in part by grant number P51 RR000167 and P40 RR019995 from the National Center for Research Resources (NCRR), a component of the National Institutes of Health (NIH), to the Wisconsin National Primate Research Center, University of Wisconsin—Madison. This research was conducted in part at a facility constructed with support from Research Facilities Improvement Program grant numbers RR15459-01 and RR020141-01.

We thank the WNPRC Virology Core for preparing the SIVmac239 inocula used in this study, the WNPRC Tetramer Core for assistance in tetramer production, and the WNPRC animal care staff. We thank David Watkins for providing samples for analysis. We also thank Chris Wright and the University of Illinois Sequencing Center. We thank members of the O'Connor lab and Tom Friedrich for their careful review of the manuscript.

REFERENCES

1. **Allen, T. M., D. H. O'Connor, P. Jing, J. L. Dzuris, B. R. Mothe, T. U. Vogel, E. Dunphy, M. E. Liebl, C. Emerson, N. Wilson, K. J. Kunstman, X. Wang, D. B. Allison, A. L. Hughes, R. C. Desrosiers, J. D. Altman, S. M. Wolinsky, A. Sette, and D. I. Watkins.** 2000. Tat-specific cytotoxic T lymphocytes select for SIV escape variants during resolution of primary viraemia. Nature **407:** 386–390.
2. **Barouch, D. H., and N. L. Letvin.** 2004. HIV escape from cytotoxic T lymphocytes: a potential hurdle for vaccines? Lancet **364:**10–11.
3. **Barouch, D. H.** 2008. Challenges in the development of an HIV-1 vaccine. Nature **455:**613–619.
4. **Burwitz, B. J., C. J. Pendley, J. M. Greene, A. M. Detmer, J. J. Lhost, J. A. Karl, S. M. Piaskowski, R. A. Rudersdorf, L. T. Wallace, B. N. Bimber, J. T. Loffredo, D. G. Cox, W. Bardet, W. Hildebrand, R. W. Wiseman, S. L. O'Connor, and D. H. O'Connor.** 2009. Mauritian cynomolgus macaques share two exceptionally common major histocompatibility complex class I alleles that restrict simian immunodeficiency virus-specific $CD8^+$ T cells. J. Virol. **83:**6011–6019.
5. **Friedrich, T. C., C. A. Frye, L. J. Yant, D. H. O'Connor, N. A. Kriewaldt, M. Benson, L. Vojnov, E. J. Dodds, C. Cullen, R. Rudersdorf, A. L. Hughes, N. Wilson, and D. I. Watkins.** 2004. Extraepitopic compensatory substitutions partially restore fitness to simian immunodeficiency virus variants that escape from an immunodominant cytotoxic-T-lymphocyte response. J. Virol. **78:**2581–2585.
6. **Hughes, A. L., H. Piontkivska, K. C. Krebs, D. H. O'Connor, and D. I. Watkins.** 2005. Within-host evolution of CD8+-TL epitopes encoded by overlapping and non-overlapping reading frames of simian immunodeficiency virus. Bioinformatics **21:**iii39–iii44.
7. **Jin, X., D. E. Bauer, S. E. Tuttleton, S. Lewin, A. Gettie, J. Blanchard, C. E. Irwin, J. T. Safrit, J. Mittler, L. Weinberger, L. G. Kostrikis, L. Zhang, A. S. Perelson, and D. D. Ho.** 1999. Dramatic rise in plasma viremia after CD8(+) T cell depletion in simian immunodeficiency virus-infected macaques. J. Exp. Med. **189:**991–998.
8. **Kawashima, Y., K. Pfafferott, J. Frater, P. Matthews, R. Payne, M. Addo, H. Gatanaga, M. Fujiwara, A. Hachiya, H. Koizumi, N. Kuse, S. Oka, A. Duda, A. Prendergast, H. Crawford, A. Leslie, Z. Brumme, C. Brumme, T. Allen, C. Brander, R. Kaslow, J. Tang, E. Hunter, S. Allen, J. Mulenga, S. Branch, T. Roach, M. John, S. Mallal, A. Ogwu, R. Shapiro, J. G. Prado, S. Fidler, J. Weber, O. G. Pybus, P. Klenerman, T. Ndung'u, R. Phillips, D. Heckerman, P. R. Harrigan, B. D. Walker, M. Takiguchi, and P. Goulder.** 2009. Adaptation of HIV-1 to human leukocyte antigen class I. Nature **458:**641–645.
9. **Keele, B. F., E. E. Giorgi, J. F. Salazar-Gonzalez, J. M. Decker, K. T. Pham, M. G. Salazar, C. Sun, T. Grayson, S. Wang, H. Li, X. Wei, C. Jiang, J. L. Kirchherr, F. Gao, J. A. Anderson, L. H. Ping, R. Swanstrom, G. D. Tomaras, W. A. Blattner, P. A. Goepfert, J. M. Kilby, M. S. Saag, E. L. Delwart, M. P. Busch, M. S. Cohen, D. C. Montefiori, B. F. Haynes, B. Gaschen, G. S. Athreya, H. Y. Lee, N. Wood, C. Seoighe, A. S. Perelson, T. Bhattacharya, B. T. Korber, B. H. Hahn, and G. M. Shaw.** 2008. Identification and characterization of transmitted and early founder virus envelopes in primary HIV-1 infection. Proc. Natl. Acad. Sci. USA **105:** 7552–7557.
10. **Loffredo, J. T., B. J. Burwitz, E. G. Rakasz, S. P. Spencer, J. J. Stephany, J. P. Vela, S. R. Martin, J. Reed, S. M. Piaskowski, J. Furlott, K. L. Weisgrau, D. S. Rodrigues, T. Soma, G. Napoe, T. C. Friedrich, N. A. Wilson, E. G. Kallas, and D. I. Watkins.** 2007. The antiviral efficacy of simian immunodeficiency virus-specific $CD8^+$ T cells is unrelated to epitope specificity and is abrogated by viral escape. J. Virol. **81:**2624–2634.
11. **Loh, L., and S. J. Kent.** 2008. Quantification of simian immunodeficiency virus cytotoxic T lymphocyte escape mutant viruses. AIDS Res. Hum. Retrovir. **24:**1067–1072.
12. **Loh, L., J. Petravic, C. J. Batten, M. P. Davenport, and S. J. Kent.** 2008. Vaccination and timing influence SIV immune escape viral dynamics in vivo. PLoS Pathog. **4:**e12.
13. **Mandl, J. N., R. R. Regoes, D. A. Garber, and M. B. Feinberg.** 2007. Estimating the effectiveness of simian immunodeficiency virus-specific $CD8^+$ T cells from the dynamics of viral immune escape. J. Virol. **81:** 11982–11991.
14. **Mothe, B. R., H. Horton, D. K. Carter, T. M. Allen, M. E. Liebl, P. Skinner, T. U. Vogel, S. Fuenger, K. Vielhuber, W. Rehrauer, N. Wilson, G. Franchini, J. D. Altman, A. Haase, L. J. Picker, D. B. Allison, and D. I. Watkins.** 2002. Dominance of CD8 responses specific for epitopes bound by a single major histocompatibility complex class I molecule during the acute phase of viral infection. J. Virol. **76:**875–884.
15. **O'Connor, D. H., A. B. McDermott, K. C. Krebs, E. J. Dodds, J. E. Miller,**

E. J. Gonzalez, T. J. Jacoby, L. Yant, H. Piontkivska, R. Pantophlet, D. R. Burton, W. M. Rehrauer, N. Wilson, A. L. Hughes, and D. I. Watkins. 2004. A dominant role for $CD8^+$-T-lymphocyte selection in simian immunodeficiency virus sequence variation. J. Virol. **78:**14012–14022.

16. **O'Connor, D. H., T. M. Allen, T. U. Vogel, P. Jing, I. P. DeSouza, E. Dodds, E. J. Dunphy, C. Melsaether, B. Mothe, H. Yamamoto, H. Horton, N. Wilson, A. L. Hughes, and D. I. Watkins.** 2002. Acute phase cytotoxic T lymphocyte escape is a hallmark of simian immunodeficiency virus infection. Nat. Med. **8:**493–499.
17. **Palmer, S., M. Kearney, F. Maldarelli, E. K. Halvas, C. J. Bixby, H. Bazmi, D. Rock, J. Falloon, R. T. J. Davey, R. L. Dewar, J. A. Metcalf, S. Hammer, J. W. Mellors, and J. M. Coffin.** 2005. Multiple, linked human immunodeficiency virus type 1 drug resistance mutations in treatment-experienced patients are missed by standard genotype analysis. J. Clin. Microbiol. **43:**406–413.
18. **Peyerl, F. W., D. H. Barouch, H. S. Bazick, E. Manuel, and N. L. Letvin.** 2005. Use of molecular beacons for rapid, real-time, quantitative monitoring of cytotoxic T-lymphocyte epitope mutations in simian immunodeficiency virus. J. Clin. Microbiol. **43:**4773–4779.
19. **Robinson, J., M. J. Waller, S. C. Fail, and S. G. Marsh.** 2006. The IMGT/HLA and IPD databases. Hum. Mutat. **27:**1192–1199.
20. **Schmitz, J. E., M. J. Kuroda, S. Santra, V. G. Sasseville, M. A. Simon, M. A. Lifton, P. Racz, K. Tenner-Racz, M. Dalesandro, B. J. Scallon, J. Ghrayeb, M. A. Forman, D. C. Montefiori, E. P. Rieber, N. L. Letvin, and K. A. Reimann.** 1999. Control of viremia in simian immunodeficiency virus infection by CD8+ lymphocytes. Science **283:**857–860.
21. **Vogel, T. U., M. R. Reynolds, D. H. Fuller, K. Vielhuber, T. Shipley, J. T. Fuller, K. J. Kunstman, G. Sutter, M. L. Marthas, V. Erfle, S. M. Wolinsky, C. Wang, D. B. Allison, E. W. Rud, N. Wilson, D. Montefiori, J. D. Altman, and D. I. Watkins.** 2003. Multispecific vaccine-induced mucosal cytotoxic T lymphocytes reduce acute-phase viral replication but fail in long-term control of simian immunodeficiency virus SIVmac239. J. Virol. **77:**13348–13360.
22. **Wang, C., Y. Mitsuya, B. Gharizadeh, M. Ronaghi, and R. W. Shafer.** 2007. Characterization of mutation spectra with ultra-deep pyrosequencing: application to HIV-1 drug resistance. Genome Res. **17:**1195–1201.
23. **Yeh, W. W., E. M. Cale, P. Jaru-Ampornpan, C. I. Lord, F. W. Peyerl, and N. L. Letvin.** 2006. Compensatory substitutions restore normal core assembly in simian immunodeficiency virus isolates with Gag epitope cytotoxic T-lymphocyte escape mutations. J. Virol. **80:**8168–8177.